Integration of sub-stoichiometric titanium oxide reactive electrochemical membrane as anode in the electro-Fenton process

Clément Trellu, Matthieu Rivallin, Sophie Cerneaux, Clémence Coetsier, Christel Causserand, Mehmet A. Oturan, Marc Cretin

HAL Id: hal-03117332
https://hal.science/hal-03117332

This is an author's version published in:
http://oatao.univ-toulouse.fr/27286

Official URL

Any correspondence concerning this service should be sent
to the repository administrator: tech-oatao@listes-diff.inp-toulouse.fr

Integration of sub-stoichiometric titanium oxide reactive electrochemical membrane as anode in the electro-Fenton process

Clément Trellu[a,b], Matthieu Rivallin[a,*], Sophie Cerneaux[a], Clémence Coetsier[c], Christel Causserand[c], Mehmet A. Oturan[b], Marc Cretin[a,*]

[a] Institut Européen des Membranes, IEM UMR 5635, Univ Montpellier, ENSCM, CNRS, Montpellier, France
[b] Laboratoire Géomatériaux et Environnement, LGE – Université Paris-Est, EA 4508, UPEM, 77454 Marne-la-Vallée, France
[c] Laboratoire de Génie Chimique, Université de Toulouse, CNRS, INPT, UPS, Toulouse, France

GRAPHICAL ABSTRACT

- TiO$_x$ REM was used for the first time as anode in EF process.
- ·OH were generated in retentate and at REM with optimal mass transport conditions.
- The efficiency of REM/EF integrated process far exceeded that of standalone processes.
- High mineralization current efficiency (77%) was obtained with REM/EF process.
- Synergy was observed from degradation in the bulk and mineralization at the TiO$_x$ REM.
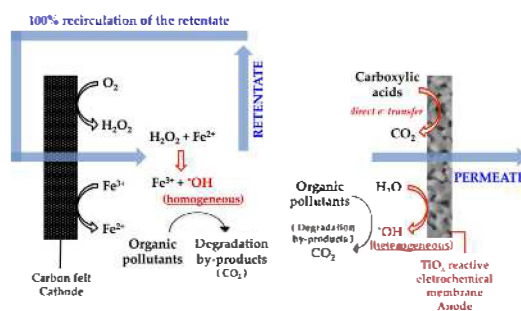
ABSTRACT

Sub-stoichiometric titanium oxide (TiO$_x$) reactive electrochemical membrane (REM) were integrated for the first time as anode in the electro-Fenton (EF) process. Hydroxyl radicals (·OH) were produced both in the retentate from Fenton's reaction and at the REM from anodic oxidation (AO). Optimal mass transport conditions were implemented because of convection-enhanced mass transport of (i) organic pollutants towards the REM surface during filtration and (ii) dissolved O$_2$ towards cathode active sites owing to the use of a 3D carbon felt cathode in flow-through configuration for H$_2$O$_2$ generation. The efficiency of the REM/EF process was much higher than EF or REM used as standalone processes. For instance, taking paracetamol as target pollutant, $(67 \pm 2)\%$ removal of 55 mg L^{-1} of initial TOC was achieved with a high mineralization current efficiency (MCE) of $(43 \pm 1)\%$. By comparison, standalone REM and EF processes achieved only 47% (MCE = 30%) and 31% (MCE = 20%) of TOC removal, respectively. By monitoring TOC removal both in retentate and permeate, the effect of homogeneous oxidation in the bulk retentate and heterogeneous oxidation at the REM could be observed separately. It was thus highlighted that the efficiency of AO might be affected by the presence of ·OH and Fe^{2+} in the bulk. It was also emphasized a synergistic effect related to the formation of carboxylic acids in the bulk retentate that are more easily mineralized at the REM where both ·OH-mediated oxidation and direct electron transfer occur.
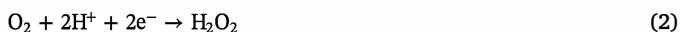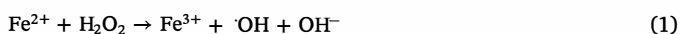
1. Introduction

Water treatment is currently a key focus for environmental engineering. In most of countries, water supply and recycling (e.g. in industrial processes) as well as protection of natural water resources are currently crucial issues. Particularly, the removal of biorefractory organic pollutants is one of the main challenges [1]. In this context, the development of electrochemical advanced oxidation processes (EAOPs) is currently a major topic of interest [2–5]. They have several technical advantages, including low (or zero) consumption of chemical reagents, process automation and compact reactor design [6,7].

EAOPs are based on the generation of hydroxyl radicals (·OH) which are able to degrade and/or completely mineralize of a wide range of biorefractory organic compounds with fast kinetics [8–17]. Firstly, ·OH can be produced homogeneously in the solution by the electro-Fenton process based on Fenton's reaction (Eq. (1)) [18–20]. Hydrogen peroxide (H_2O_2) is generated by the two-electron reduction of dissolved O_2 at carbon-based cathodes (Eq. (2)), while a catalytic amount of ferrous iron is sufficient to start the Fenton's reaction (Eq. (3)). Then, Fe^{2+} ion (catalyst) is generated/regenerated at the cathode from reduction of Fe^{3+} formed in Eq. to ensure continuous generation of ·OH (Eq. (3)) [21]. Secondly, ·OH can be also generated heterogeneously (AO) through water oxidation at the surface of anodes with high overpotential for oxygen evolution reaction (Eq. (4)) [7,22–25].

$$Fe^{2+} + H_2O_2 \rightarrow Fe^{3+} + \cdot OH + OH^- \tag{1}$$

$$O_2 + 2H^+ + 2e^- \rightarrow H_2O_2 \tag{2}$$

$$Fe^{3+} + e^- \rightarrow Fe^{2+} \tag{3}$$

$$M + H_2O \rightarrow M(\cdot OH) + H^+ + e^- \tag{4}$$

The electron is the main reagent during EAOPs, thus the Faraday efficiency is a crucial parameter for assessing process efficiency [7]. Parasitic and wasting reactions must be minimized so that the electrons supplied to the system are used effectively for the degradation and mineralization of pollutants. Because of the short lifetime of ·OH, low Faraday efficiency usually results from mass transport limitations [2,26,27]. For example, anodic oxidation (AO) is a heterogeneous electro-catalytic process during which physisorbed ·OH are generated at the anode surface, thus resulting in a thin reactive layer close to the anode surface (less than 1 μm). Therefore, process efficiency is often limited by the diffusion boundary layer at the solution/electrode interface ($\approx$100 μm) [27]. Recently, the use of sub-stoichiometric titanium oxide (TiO_x) reactive electrochemical membrane (REM) as anode has been developed [27–33]. Such anode material is able to strongly enhance current efficiency because of the higher electro-active surface area and convection-enhanced mass transport of pollutants from the bulk to the anode in flow-through operation [27,29,33,34]. Such material also represents a promising alternative to boron-doped diamond electrodes for reducing capital expenditures of electrochemical systems [35]. Besides, H_2O_2 production for the EF process can be also limited by mass transport issues because of the low solubility of O_2 in water. Thus, recent studies have developed 3D flow-through carbon-based cathode for production of large amounts of H_2O_2 [36–39]. The objective is to improve mass transport of dissolved O_2 to cathode active sites.

In the present study, it is proposed for the first time, the integration of TiO_x REM as anode in the EF process. 3D flow-through carbon felt (CF) was used as cathode. The objective is to achieve mineralization of organic compounds with high current efficiency owing to optimal mass transport conditions. Optimal conditions for H_2O_2 production were identified and the efficiency of various configurations (REM alone, EF alone, REM/H_2O_2 and REM/EF) for the removal of a model pharmaceutical residue (paracetamol) were compared in order to emphasize the suitability of the new REM/EF process. Moreover, by using TiO_x REM as anode and without recirculation of the permeate, it was possible to well differentiate the oxidation of organic compounds by either

homogeneous reactions in the bulk (TOC removal in the retentate) or heterogeneous reactions at the TiO_x REM (TOC removal between retentate and permeate). Thus, this study allowed the identification for the first time of antagonist and synergistic phenomena occurring when EF and AO processes are integrated into a single reactor.

2. Materials and methods

2.1. Chemicals

All chemicals were of reagent grade and purchased from Sigma Aldrich. Aqueous solutions were prepared with deionized water (R > 18 MΩ cm).

2.2. Electrode materials

Anode materials were TiO_x REM supplied by Saint-Gobain Research Provence (CREE Cavaillon, France). This porous material was synthesized from carbothermal reduction of TiO_2 by using an extrusion die, based on the method developed by Saint-Gobain Research Provence. The synthesis method starts from a mixture of anatase TiO_2, carbon black, organic binders and water. Then a debinding step followed by a sintering and carbothermal reduction step performed during 2 h at 1300 °C under argon atmosphere allows for the formation of this porous material. Additional details on the synthesis method are provided in Trellu et al. (2018) [28]. These anodes are a mixture of Ti_4O_7 and Ti_5O_9 Magnéli phases. They have a monodispersed pore size distribution, with a median pore size of 1.4 μm, a porosity (pore volume) of 41% and a specific surface area of 0.40 m^2 g^{-1}. The water permeability of these TiO_x membranes is 3300 L m^{-2} h^{-1} bar^{-1}. The characteristics of materials obtained were detailed Trellu et al. (2018) [28] (scanning electron microscopy images, HF intrusion porosimetry and X-ray diffraction data are provided as Supplementary Material). Electrodes were stable in the range of current density and exploitation duration required for this study. Long-term stability tests are the focus of on-going studies. Cathode materials were 6.35 mm thick CF supplied by Alfa Aesar.

2.3. Experimental installation

The schematic diagram of the experimental installation is shown in Fig. 1.

TiO_x REM (inside/outside diameter = 6/10 mm, active outer surface 27.6 cm^2) was used as anode with the solution flowing from the outside (retentate) to the inside (permeate) of the tube. CF cathode (15 × 8 cm^2, 6.3 mm thick) was placed concentrically around the REM with an inter-electrode distance of 3.5 cm. O_2 was injected in the tank
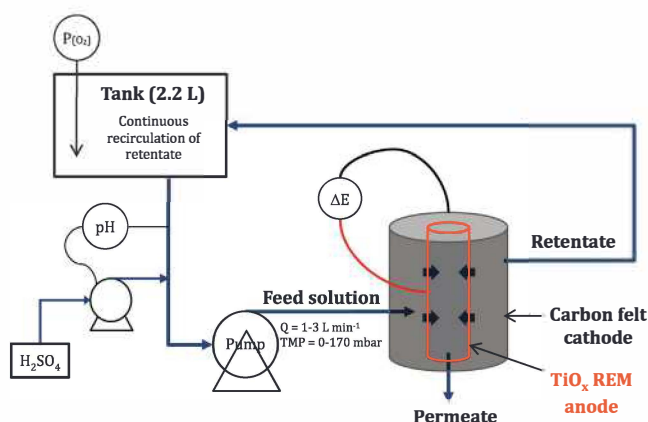

Fig. 1. Scheme of the experimental installation (without recirculation of the permeate) equipped with a tubular anodic TiOx REM and a cathodic carbon felt placed concentrically around the REM in the retentate compartment.

by bubbling fine bubbles of O_2 in the solution. Experiments were carried out with paracetamol (PCT) as a model organic pollutant with initial total organic carbon content (TOC_0) of 55 or 110 mg L^{-1}. Sodium sulfate at low concentration (5 mM) was used as supporting electrolyte. The total volume of the treated solution was 2.2 L for all experiments (meaning that the ratio between the geometric surface area of the anode and the volume of solution was 0.0125 cm^{-1}). For the EF process, 0.2 mM of Fe^{2+} was initially added to the solution to be treated. The pH was initially adjusted to 3.0 with H_2SO_4, in accordance with the optimal pH for the EF process [6]. An injection system of H_2SO_4 in the retentate, controlled by a pH regulation, maintained the pH value between 2.9 and 3.1 in the retentate during operation of EF without recirculation of the permeate.

The process was operated without continuous feed of the reactor and the retentate was continuously recirculated at 100% for all experiments. When entering the electrochemical cell, the solution is first forced to flow through the CF cathode. Then, a portion of the solution flows through the REM according to the transmembrane pressure (TMP) and is collected as permeate. The rest of the solution is forced to flow again through the CF before to come back to the feed tank. A recirculation pump was used to adjust the retentate recirculation flow rate in the range of Q = 1–3 L min^{-1}). TMP was in the range 0–170 mbar. The experiments were carried out either by continuously collecting the permeate or by recirculating the permeate at 100% in the feed tank (retentate). All experiments were carried out in galvanostatic mode, using an ELC power supply (AL924A). The current density (j) was adjusted between 6 and 30 mA cm^{-2} (always calculated from the geometric surface of the anode). The experiments were conducted systematically for 5 h.

Different processes have been tested depending on operating conditions, which are given in Table 1:

2.4. Analytical procedures

PCT concentration was measured by HPLC (Agilent 1200 system) with C18 column and UV detector (λ = 254 nm). The mobile phase was a mixture of water and acetonitrile containing 0.1% v/v formic acid. HPLC was operated at a constant flow rate of 1.0 mL min^{-1} using a gradient elution as described previously [40].

TOC was measured with a Shimadzu TOC-L analyzer using the catalytic oxidation combustion method at 680 °C. The relative standard deviation on TOC measurements was 2%. Percentage of TOC removal in the retentate at time t was calculated using Eq. (5). Percentage of TOC removal in the permeate at time t was calculated using Eq. (6). Global percentage of TOC removal (taking into consideration TOC removal in both retentate and permeate) at the end of the experiment was calculated using Eq. (7).

$$\text{TOC removal in the retentate (t) (\%)} = \left(1 - \frac{TOC_{ret,t}}{TOC_0}\right) \times 100 \tag{5}$$

$$\text{TOC removal in the permeate (t) (\%)} = \left(1 - \frac{TOC_{per,t}}{TOC_{ret,t}}\right) \times 100 \tag{6}$$

Global TOC removal (%)
$$= \left(1 - \frac{(TOC_0 - TOC_{per}) \times V_{per} + (TOC_0 - TOC_{ret}) \times V_{ret}}{TOC_0 \times V_0}\right) \times 100 \tag{7}$$

where $TOC_{ret,t}$ and $TOC_{per,t}$ are TOC concentrations in the retentate and permeate at time t, and 0 (initial concentration); TOC_{ret} and TOC_{per} are TOC concentrations in the retentate and permeate at the end of the experiment; TOC_0 is the initial concentration of TOC; V_{ret} and V_{per} are the volumes of retentate and permeate at the end of the experiment; V_0 is the initial volume of the feed solution.

Mineralization current efficiency (MCE) was calculated using the following equation (Eq. (8)) for assessing the Faraday efficiency of the process for mineralization of PCT.

$$\text{MCE(\%)} = \frac{\Delta TOC_{exp}}{\Delta TOC_{th}} \times 100 \tag{8}$$

where ΔTOC_{exp} is the amount of TOC removed during experiments and ΔTOC_{th} is the theoretical TOC removal calculated by assuming that the electrical charge was only consumed for mineralization of PCT.

H_2O_2 electrochemically generated in the retentate was analyzed by a spectrophotometric method, based on the measurement of the absorbance at 410 nm of a colored complex (titanium peroxysulfate) formed in the presence of Ti^{4+} in sulfuric acid medium [41]. Current efficiency for H_2O_2 production was calculated similarly to MCE, based on the amount of H_2O_2 measured during experiments and the theoretical amount of H_2O_2 that could be produced by assuming that the electrical charge was only consumed for the two electron reduction of O_2 (Eq. (2)). Accumulation rate of H_2O_2 was calculated using Eq. (9).

H_2O_2 accumulation rate (t_i) (mg min^{-1})
$$= \frac{[H_2O_2]_{t_i} \cdot V_{ret,t_i} - [H_2O_2]_{t_{i-1}} \cdot V_{ret,t_{i-1}}}{t_2 - t_1} \tag{9}$$

where $[H_2O_2]_{ti}$ and $[H_2O_2]_{ti-1}$ are concentrations in mg L^{-1} at time t_i and t_{i-1} (min), respectively. Similarly, $V_{ret,ti}$ and $V_{ret,ti-1}$ are the volumes of retentate (L) at time t_i and t_{i-1}, respectively.

Oxamic acid was identified and quantified by ion-exclusion HPLC equipped with a BENSON column (300 mm, 7.8 mm (i.d.)) and using a refractive index detector (Waters 2414). Column temperature was set at 30 °C. A solution of 1.5 mM H_2SO_4 was used as mobile phase with isocratic elution at 0.4 mL min^{-1}.

Some experiments were carried out in triplicate in order to assess the reproducibility of experimental data.

3. Results and discussion

3.1. H_2O_2 production

The first set of experiments aimed at evaluating the capacity of the

Table 1
Operating conditions used for the different processes. The feed/retentate recirculation flow rate was controlled at Q = 1 L min^{-1} for all configurations. TMP: transmembrane pressure; EF: electro-Fenton; REM: reative electrochemical membrane.

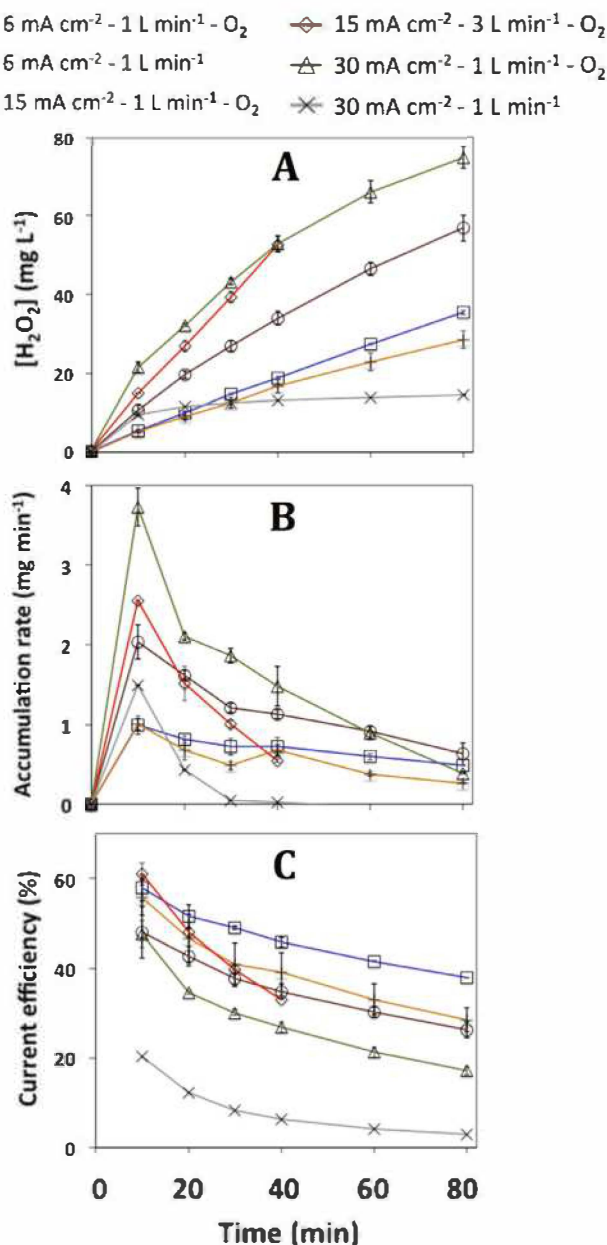| Process	TMP (mbar)	O_2 supply	[Fe^{2+}] (mM)
EF	0	yes	0.2
Electro-Fenton in the bulk retentate with low anodic oxidation at the REM	(no permeate flux)		
REM	30	no	0
Anodic oxidation at the REM			
REM/H_2O_2	30	yes	0
AO at the REM and generation of H_2O_2 in the bulk retenate			
REM/EF	30	yes	0.2
Electro-Fenton in the bulk retentate and AO at the REM			

Fig. 2. Evolution over time of: (A) concentration of H_2O_2 in the retentate, (B) accumulation rate (mg min^{-1}) of H_2O_2 in the retentate and (C) current efficiency for accumulation of H_2O_2 in the retentate, as a function of current density (j = 6, 15 or 30 mA cm^{-2}, corresponding to 1.4, 3.5 or 6.9 mA cm^{-2} for the carbon felt cathode), recirculation flow rate of the retentate (Q = 1 or 3 L min^{-1}) and O_2 supply (with or without). All experiments have been performed in deionized water with 5 mM of Na_2SO_4. Data above 40 min have not been measured for the experiment at 3 L min^{-1} because of the higher TMP that decreased rapidly the volume of the retentate. Error bars have been calculated from replicate experiments (n = 3).

system to produce H_2O_2 for the EF process, according to current density, recirculation flow rate and O_2 supply. Results are presented in Fig. 2. Generation of H_2O_2 is based on dissolved O_2 reduction at the cathode. At low current density (6 mA cm^{-2}), the consumption of dissolved O_2 was low (Fig. 2A). Therefore, O_2 supply only slightly increased H_2O_2 production rate because O_2 transfer from the gas phase to the liquid phase into the tank was almost sufficient to counterbalance O_2 reduction at the cathode. However, at high current density (30 mA cm^{-2}), O_2 reduction rate at the cathode was strongly increased. Without O_2 supply, H_2O_2 accumulation rate rapidly decreased to 0. In

fact, the concentration remained constant after 30 min of operation while the volume of retentate was continuously decreasing; therefore the amount of H_2O_2 in the reactor was actually lower at 80 min than at 30 min. These results highlight that O_2 supply is mandatory for maintaining the H_2O_2 production rate.

For all experiments with O_2 supply, the accumulation rate of H_2O_2 decreased with time. experiment. (Fig. 2B). Generation of H_2O_2 was assumed to be constant during experiments since O_2 was supplied in excess. However, the accumulation of H_2O_2 comes from the difference between generation and destruction of H_2O_2. In this configuration, destruction of H_2O_2 can be ascribed to both cathodic reduction (Eq. (10)) and anodic oxidation (Eq. (11)). These reactions are promoted at high H_2O_2 concentration, explaining thus the decrease of H_2O_2 accumulation rate during all experiments as well as the stronger relative decrease of H_2O_2 accumulation rate with time when operating the process at high current density (for which higher concentration of H_2O_2 was reached).

$$H_2O_2 + 2H^+ + 2e^- \rightarrow 2H_2O \tag{10}$$

$$H_2O_2 \rightarrow O_2 + 2H^+ + 2e^- \tag{11}$$

After operating the process during 30 min at 30 mA cm^{-2} (corresponding to 6.9 mA cm^{-2} for the CF cathode), (79 $\pm$ 2) mg of H_2O_2 was accumulated in the retentate (2.2 L). In a recent study of Pérez et al. (2016) reported the accumulation of around 260 mg of H_2O_2 (in 1 L) after 30 min using polytetrafluoroethylene-modified carbon felt at 50 mA cm^{-2} [36]. The Venturi-based jet cell used in this study was reported to be as efficient as conventional gas diffusion electrode. By comparing these results, one can conclude that the system developed in the present study seems to be highly competitive, since the amount of H_2O_2 accumulated was only 3.3 times lower by using a current density 7.2 times lower with a non-modified carbon felt cathode.

High current efficiency for H_2O_2 production (between 30 and 50% after 30 min) was observed whatever the current density applied for experiments performed with O_2 supply (Fig. 2C). The high efficiency of the reactor was ascribed to operation of the process under flow-through mode with continuous recirculation of the retentate through the CF cathode, thus allowing a convection-enhanced mass transport of dissolved O_2 to cathode active sites [36].

The influence of this convection-enhanced mass transport was further investigated by increasing the recirculation flow rate from 1 to 3 L min^{-1} for experiments performed at 15 mA cm^{-2} and with O_2 supply (Fig. 2). Higher recirculation flow rate increased the TMP (30 mbar at 1 L min^{-1} and 170 mbar at 3 L min^{-1}), and subsequently, the permeate flux through the REM (95 L h^{-1} m^{-2} at 1 L min^{-1} and 510 L h^{-1} m^{-2} at 3 L min^{-1}). Within the first minutes, higher current efficiency was observed ((61 $\pm$ 1)%) at 3 L min^{-1} compared to 1 L min^{-1} ((48 $\pm$ 4)%) owing to the promotion of the convection-enhanced mass transport of dissolved O_2 towards cathode active sites. However, no significant difference of current efficiency was then observed after 40 min. In fact, higher recirculation flow rate and higher permeate flux through the TiOx REM used as anode also favored H_2O_2 destruction following Eqs. (10) and (11), respectively. Moreover, the higher concentration reached at the beginning of the experiment also promoted H_2O_2 destruction following Eq. (10) and Eq. (11).

As regards to the influence of current density, higher accumulation rate of H_2O_2 was obtained at the beginning of experiments performed at high current density. However, the accumulation rate then strongly decreased with time and the current efficiency was also lower compared to experiments performed at lower current density because of the promotion of parasitic reactions involving either H_2O_2 destruction (Eqs. (10) and (11)) or hydrogen evolution reaction (Eq. (12)).

$$2H^+ + 2e^- \rightarrow H_2 \tag{12}$$

Overall, sustainable operating conditions for H_2O_2 production in the retentate during the REM/EF process were identified as

$j = 15$ mA cm^{-2} (intermediate current density), continuous O$_2$ supply and $Q = 1$ L min^{-1}. The choice of the recirculation flow rate was also selected as regards to its influence on the TMP. In fact, successful operation of the REM/EF process is based on the selection of the best compromise in terms of optimizing operating conditions for both electrochemical formation of the Fenton's reagent in the retentate and AO at the TiO$_x$ REM. As regards to the efficiency of AO, it tightly depends on permeate and TOC flux through the TiO$_x$ REM. Previous study on TiO$_x$ REM revealed that optimal MCE for mineralization of PCT at 15 mA cm^{-2} was obtained for TOC flux through the REM in the range 5–15 g m^{-2}h^{-1} [28]. By using a recirculation flow rate of 1 L min^{-1} involving a TMP of 40 mbar, TOC flux through the REM could be adjusted to 5.2 and 10.4 g m^{-2}h^{-1} when performing experiments with TOC$_0$ = 55 and 110 mg L^{-1}.

3.2. Process efficiency

The objective of the following experiments was to evaluate the relevance and effectiveness of the innovative integrated process, by comparing the TOC removal (mineralization) achieved with the different configurations, i.e., EF standalone process, REM standalone process, REM/H$_2$O$_2$ process and REM/EF integrated process (Fig. 3). Experiments were carried out considering the optimal conditions justified in section 3.1. Experiments were performed either without recirculation of the permeate or with 100% recirculation of the permeate (meaning in this case that the volume of the retentate was constant throughout the experiment, similarly to a batch experiment) and at two different TOC concentrations (TOC$_0$ = 55 or 110 mg L^{-1}).

All values of percentage of TOC removal have been calculated by taking into consideration TOC removal in both retentate and permeate (Eq. (7)). For example, for the REM configuration with TOC$_0$ = 55 mg L^{-1}, the percentage of TOC removal calculated from the difference between TOC in retentate and permeate was (90 ± 2)% (Eq. (6)). However, after 5 h of treatment, the total volume of permeate (filtrated water that passed through the REM) was 1 L. Thus, mineralization in the permeate resulted in a global percentage of TOC removal of only 41% by taking into consideration the total volume of the effluent (V$_0$ = 2.2 L).

Overall, the global percentage of TOC removal (ascribed to mineralization in both retentate and permeate, as described in Eq. (7)) with the REM configuration was only slightly higher (47%) because low mineralization was simultaneously achieved in the retentate (non-filtrated water). In fact, very low amount of oxidizing species was generated in the bulk because of the absence of O$_2$ supply for H$_2$O$_2$ production and absence of Fe^{2+} for production of ·OH according to Eq. (3). By comparison, slightly higher global percentage of TOC removal was obtained with the REM-H$_2$O$_2$ configuration because O$_2$ supply enhanced H$_2$O$_2$ production in the retentate, which participated to oxidation of organics (TOC removal in the retentate was increased from 3 to 10% after 5 h). The best way to further promote the oxidation of organic pollutants in the retentate was to implement EF by supplying both O$_2$ and 0.2 mM of Fe^{2+} in order to generate large amounts of ·OH in the retentate. Thus, EF alone achieved 31% removal of TOC after 5 h of treatment. Interestingly, the highest effectiveness was achieved with the integrated process REM/EF: the global percentage of TOC removal reached (67 ± 2)%. This value was 1.4 and 2.2 times higher than that obtained with REM alone and EF alone, respectively.

The efficiency of the integrated process was further highlighted by the high MCE obtained. The MCE achieved during the treatment of the solution at TOC$_0$ = 55 mg L^{-1} was (43 ± 1)%. MCE was even further increased to 77% for the treatment of the solution at TOC$_0$ = 110 mg L^{-1}. In fact, wasting reactions at high current intensity (reaction of ·OH with non-organic compounds, its dimerization to H$_2$O$_2$ (Eq. (13)) or reaction with Fe^{2+} (Eq. (14)) are further hindered at high concentration of organic matter. These values of MCE are higher than in previously published studies on EF process in batch reactor using plate boron-doped diamond or TiO$_x$ anode [25,42–45]. For example, Ganiyu et al. (2019) reported a lower efficiency during electro-oxidation of PCT by EF using Ti$_4$O$_7$ anode. The MCE was 6% for 70% removal of 30.2 mg L^{-1} of PCT by using plate electrode in batch reactor with a current density of 5 mA cm^{-2} and a ratio between the geometric surface area of the anode and the volume of solution of 0.10 cm^{-1} [45]. In fact, electrochemical advanced oxidation processes using plate electrodes (EAOPs) are usually operated under mass transport limitation [7,26]. By comparison, the great advantage of this REM/EF process is the enhancement of the mass transport of (i) organic pollutants from the bulk to the anode surface by convection during filtration through the REM with low pore size [27,28,30] and (ii) dissolved O$_2$ from the bulk to CF cathode active sites (for H$_2$O$_2$ generation) owing to flow-through operation with continuous recirculation of the retentate through the CF cathode [36].
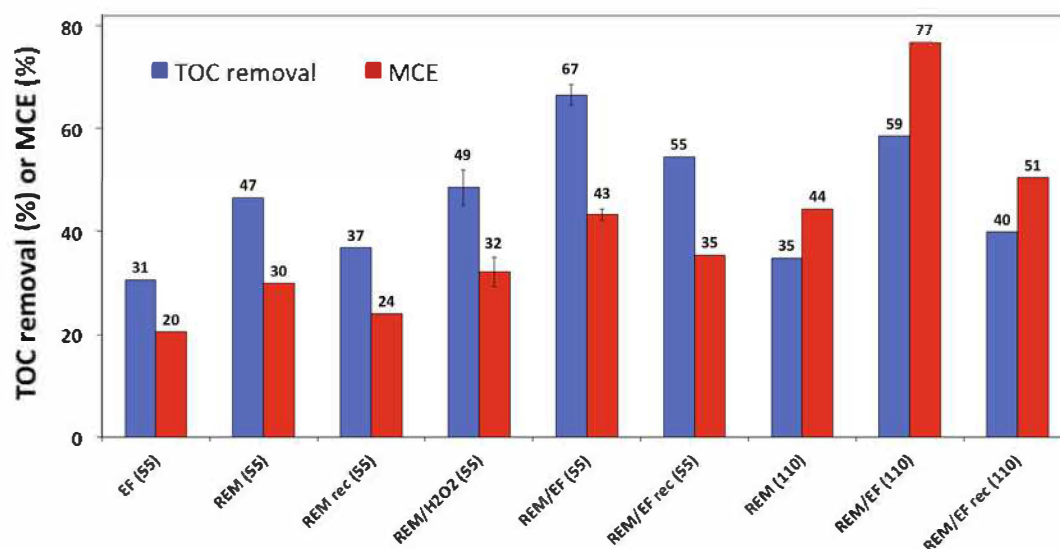

Fig. 3. Global percentage of TOC removal and MCE (%) as a function of experimental configuration (EF standalone process, REM standalone process, REM/H$_2$O$_2$ process, or integrated REM/EF process) and initial TOC concentration of the paracetamol solution (TOC$_0$ = 55 or 110 mg L^{-1}). REM/EF rec are the experiments performed with 100% recirculation of the permeate. Error bars for REM/H$_2$O$_2$ and REM/EF have been calculated from replicate experiments (n = 3). Calculations have been made using Eqs. (7) and (8).

$$\cdot OH + \cdot OH \rightarrow H_2O_2 \tag{13}$$

$$Fe^{2+} + \cdot OH \rightarrow Fe^{3+} + OH^- \tag{14}$$

Experiments were also carried out by continuously recirculating the permeate into the retentate during REM/EF experiments. Therefore, similarly to a batch experiment, the total volume in the retentate remained constant throughout the experiment. TOC removal was 1.2 and 1.5 times lower compared experiments performed without recirculation at $TOC_0 = 55$ and 110 mg L^{-1}, respectively. This lower effectiveness was due to a faster decrease of the TOC in the retentate (because of the recirculation of the permeate with low TOC content), which further promoted wasting reactions (Eqs. (10) and (11)). However, the advantage of this configuration was related to pH control. Water reduction at the cathode generates HO^- and caused a significant pH increase in the retentate (pH = 11.8 after 5 h) when the process was performed without recirculation of the permeate. In this configuration, a pH regulation using H_2SO_4 was therefore required for implementing the EF process in the retentate at pH between 2.9 and 3.1. Besides, water oxidation at the anode generates H^+ that resulted in a strong decrease of the pH in the permeate (pH = 2.1). Overall, it was observed that operating the process with continuous recirculation of the permeate keeps the pH in the retentate between 2.9 and 3.1 throughout the experiment, without adding H_2SO_4. Indeed, H^+ generated at the anode neutralized the effect of HO^- generated at the cathode. Besides, as regards to the continuous operation of such reactor, pH regulation would depend on the way to implement the process (continuous feed of polluted water, partial recirculation of the permeate, etc.)

3.3. Electro-oxidation mechanisms

During the EF process, oxidant species can be generated either homogenously in the retentate (Eqs. (1)–(3)) or heterogeneously at the anode if a suitable electrode material is used (Eq. (4)). Different oxidation mechanisms are therefore involved, resulting in different behaviors in terms of degradation and mineralization kinetics. While degradation only refers to the initial oxidation of PCT, mineralization involves a complete destruction of organic compounds into inorganic species. While results presented in section 3.1 and 3.2 gave information on the global mineralization effectiveness achieved, the objective of the following experiments was to emphasize the differences in electro-oxidation mechanisms ascribed to homogeneous oxidation in the bulk and heterogeneous oxidation at the TiO_x REM.

First, the evolution of both PCT ($[PCT]_0 = 87$ mg L^{-1}) and TOC concentrations ($TOC_0 = 55$ mg L^{-1}) was monitored over time when using REM and REM/EF configuration with continuous permeate recirculation (Fig. 4). With the REM configuration, it is interesting to observe that degradation and mineralization kinetics were very similar. This can be explained by the complete and fast mineralization of organic pollutants near the anode surface due to the production of large amounts of M($\cdot OH$) at the anode surface. Compared to plate anodes in batch experiments, the use of REM further favors the complete mineralization of organics since the oxidation process is focused on the small volume of solution passing through the REM, without back diffusion of molecules from the anode surface to the bulk. In fact, a single passage through the REM achieved 90% removal of TOC between permeate and retentate (Fig. 5). Besides, with the REM configuration, almost none oxidant species was generated in the retentate, thus avoiding PCT degradation in the retentate. Overall, the benefit of this configuration thus lies in the very low production and accumulation of degradation by-products that can be sometimes more toxic than initial molecules. Such phenomenon usually requires high current density for conventional plate anodes and results in low current efficiency because of mass transport limitations [7,26]. However, with this configuration, high MCE (24%) was maintained for 37% TOC removal thanks to the convection enhanced mass transport of pollutants towards the REM used as anode.
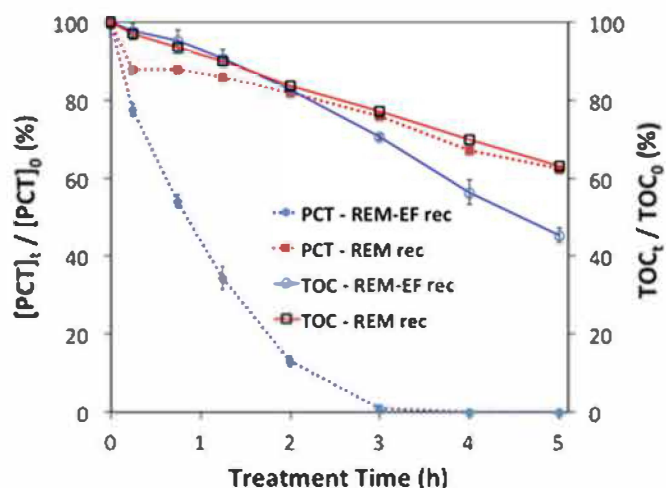

Fig. 4. PCT ($[PCT]_0 = 87$ mg L^{-1}) and TOC evolutions ($TOC_0 = 55$ mg L^{-1}) evolution over time, as a function of the experimental configuration (REM standalone process or integrated REM/EF process). All experiments have been performed with continuous recirculation of the permeate. Error bars for REM/EF have been calculated from replicate experiments (n = 3). Calculations have been made using Eq. (5).

During the REM/EF process, faster degradation kinetic of PCT was observed compared to mineralization (Fig. 4). Data obtained for PCT degradation during the REM/EF process fit well with the pseudo-first order model ($R^2 = 0.997$) with an apparent rate constant of 0.84 h^{-1}. In the previous study of Brillas et al. (2005), similar rate constant was obtained (0.78 h^{-1}) during AO using BDD anode. However, the current density was much higher (100 mA cm^{-2} compared to 15 mA cm^{-2} in this study) and the ratio between the geometric surface area of the anode and the volume of solution was also higher 0.030 cm^{-1} (compared to 0.0125 cm^{-1} in this study). Homogeneous production of $\cdot OH$ from electrochemically generated Fenton's reagent strongly improved the degradation of PCT in the retentate. In fact, > 99% of PCT was degraded after 3 h of treatment, while only 38% of PCT was degraded after 5 h of treatment by the REM process alone. Combination of REM with the EF process also increased the removal of TOC from 37 to 55% and the MCE from 24 to 35% after 5 h of treatment. The benefit of this configuration lies in the higher effectiveness for degradation and mineralization of PCT because of production of oxidant species both homogeneously in the bulk retentate and heterogeneously at the surface of the REM. Besides, the much faster degradation of PCT compared to the mineralization kinetic means that degradation by-products are accumulated in the solution. Recent studies have highlighted the possibility to combine the EF process with a biological post-treatment for cost-effective biodegradation of degradation by-products [46–49]. In this context, the REM/EF configuration would be much more suitable than the REM configuration.

Fig. 5A shows the evolution over time of TOC concentration in permeate and retentate during experiments with $TOC_0 = 55$ mg L^{-1}. From TOC measurement in the retentate it is possible to observe electro-oxidation ascribed to homogeneous oxidation in the bulk, while heterogeneous oxidation at the REM can be observed from TOC removal between retentate and permeate. A similar trend was obtained for both REM and REM/H_2O_2 configurations. TOC concentration decreased very slowly in the retentate because of the absence of homogeneous $\cdot OH$ generation. Besides, the analysis of TOC in the permeate revealed that the effectiveness of the REM for PCT mineralization remained constant throughout the 5 h of treatment. In the case of the REM/EF integrated process, TOC concentration in the retentate decreased quickly due to the production of $\cdot OH$ formed via Fenton's reaction (Eq. (2)). However, at the beginning of the experiment, the effectiveness of heterogeneous oxidation at the REM was lower in the
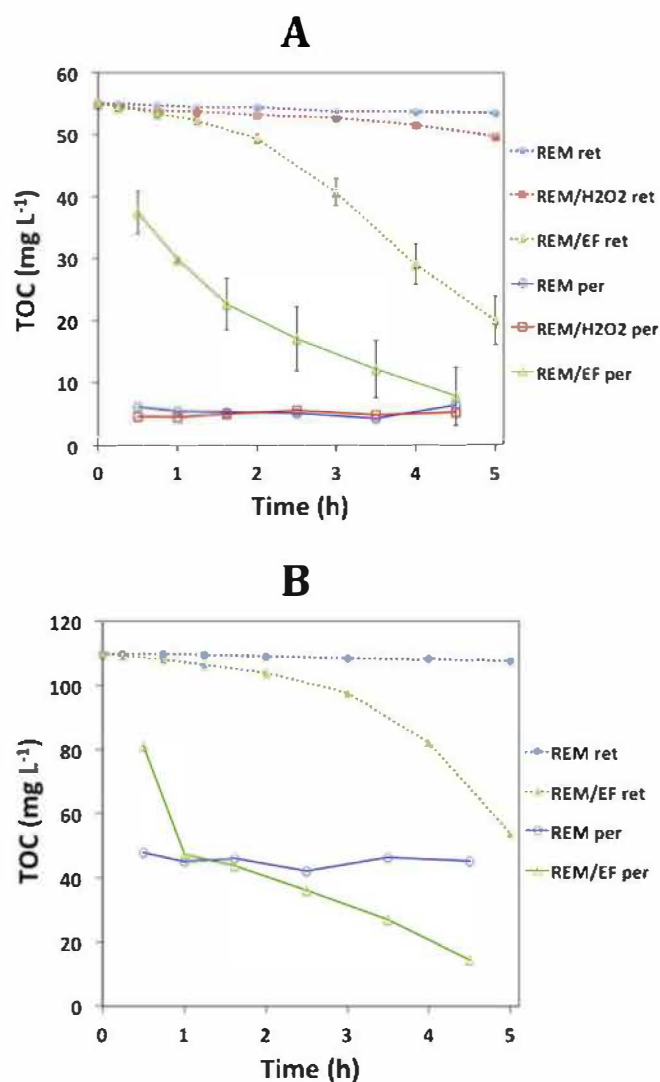
A

B

Fig. 5. TOC evolution over time, as a function of the experimental configuration (REM standalone process, REM/H₂O₂ process, or integrated REM/EF process). (A) $TOC_0 = 55$ mg L^{-1} and (B) $TOC_0 = 110$ mg L^{-1}. All experiments have been performed without recirculation of the permeate. "ret" refers to concentrations analyzed in the retentate, while "per" refers to concentrations analyzed in the permeate. Error bars for REM/EF have been calculated from replicate experiments (n = 3). Calculations have been made using Eqs. (5) and (6).

configuration REM/EF compared to the configuration REM alone (without generation of ·OH in the retentate). TOC removal at the REM by the REM/EF was only 32% at t = 0.5 h of treatment with the REM/EF configuration, compared to 90% with the configuration REM. This phenomenon could be attributed to the promotion of wasting reactions at the REM surface during filtration of the retentate containing ·OH and Fe^{2+} in the case of the REM/EF configuration. These wasting reactions are more specifically (i) the dimerization reaction between ·OH homogeneously produced in the retentate and ·OH heterogeneously produced from AO at the REM (Eq. (13)) and (ii) the reaction of ·OH heterogeneously produced at the REM with Fe^{2+} ions present in the retentate (Eq. (14)).

Similarly, a lower effectiveness of the REM at the beginning of the treatment with the REM/EF process compared to the configuration with the REM alone was observed during experiments performed at initial TOC of 110 mg L^{-1} (Fig. 5B). However, with this higher TOC concentration, the presence of ·OH and Fe^{2+} in the retentate had a lower impact on TOC removal by heterogeneously produced ·OH at the REM.

First, this phenomenon might be ascribed to a lower steady-state concentration of ·OH in the retentate because of further reaction of homogeneously generated ·OH with a greater amount of TOC. Furthermore, there is actually a competition between the different species in the retentate (organic compounds, homogeneously generated ·OH and Fe^{2+}) for reaction with heterogeneous ·OH generated at the REM. By increasing the TOC concentration in the retentate, the reaction between heterogeneous ·OH and organic compounds might be promoted, thus decreasing wasting reaction of heterogeneous ·OH with Fe^{2+} and homogeneously generated ·OH.

Interestingly, with the REM/EF configuration, it was observed that the reaction in the retentate strongly improved the effectiveness of the heterogeneous reaction at the REM. For example, during the experiment with $TOC_0 = 55$ mg L^{-1}, TOC removal by the REM increased from 32% at t = 0.5 h to 57% at 1.6 h of treatment (values calculated from TOC data given in Fig. 5; details of these results are provided as Supplementary Material), while TOC removal in the retentate was less than 10% in the same time. Even more significant, during the experiment at $TOC_0 = 110$ mg L^{-1}, TOC removal by the REM increased from 26% at t = 0.5 h to 59% at t = 1.6 h, while TOC removal in the retentate was less than 6% in the same time. These results indicate a strong synergistic effect between the EF process and the use of TiO_x REM as anode. The EF process is well known for producing rapidly short-chain carboxylic acids as degradation by-products of aromatic organic pollutants, particularly oxalic and oxamic acids in the case of PCT [50]. In this study, oxamic acid was used as a model molecule for carboxylic acid compound in order to assess the fate of such components. A high concentration of 23 mg L^{-1} was detected in the retentate after 5 h of treatment with the REM/EF configuration ($TOC_0 = 55$ mg L^{-1}). By comparison, only 2.5 mg L^{-1} of oxamic acid was detected in the permeate with the REM configuration (same TOC_0). Compared to aromatic compounds, carboxylic acids have lower rate constants for reaction with ·OH homogeneously produced in the bulk. However, TiO_x REM is able to quickly oxidize such compound by direct electron transfer [29,30]. Therefore, when using TiO_x REM as anode, both ·OH-mediated oxidation and direct electron transfer can occur simultaneously [27,29,30]. Thus, such anode material is particularly suitable for improving the removal of carboxylic acids and the mineralization efficiency of the EF process.

The antagonist and synergistic phenomena occurring during the combination of homogeneous electro-oxidation (in the bulk retentate by electrochemically produced Fenton's reagent) and heterogeneous electro-oxidation (at the TiO_x REM by AO) is highlighted for the first time in this configuration allowing the separation of oxidation mechanisms in the bulk retentate and at the anode/REM.

4. Conclusions

Optimal conditions for removal of PCT ($TOC_0 = 55$ or 110 mg L^{-1}) by the REM/EF integrated process were selected as (i) j = 15 mA cm^{-2} (ii) recirculation flow rate of 1 L min^{-1} involving TMP = 30 mbar and J = 95 L h^{-1} m^{-2} and (iii) continuous O_2 supply. Very high efficiency of this process was obtained for mineralization of PCT solution (e.g., 59% removal of 110 mg L^{-1} of TOC with MCE = 77%) because of favorable mass transport conditions for (i) H_2O_2 production owing to the flow-through operation mode with continuous recirculation of the retentate through the CF cathode and (ii) electro-oxidation of organic compounds at the TiO_x REM owing to the convection-enhanced mass transport of pollutants during filtration through the REM. Such conditions allow taking advantage of the high electro-active surface area of these three dimensional porous electrodes.

The configuration REM/EF allowed for the first time the separation of oxidation mechanisms in the bulk retentate and at the anode/REM. An antagonist effect was observed during filtration of the bulk retentate through the REM because of wasting reactions of ·OH heterogeneously produced at the REM with ·OH homogeneously produced in the

retentate as well as with Fe^{2+} ions. However, a strong synergistic effect was also emphasized between the degradation of PCT in the retentate by homogeneous ·OH and the complete mineralization of degradation by-products at the REM. In fact, direct electron transfer can also occur at the TiO_x REM and degradation by-products such as carboxylic acids are more easily mineralized by direct electron transfer than by oxidation with homogeneous ·OH. This phenomenon also explains why the overall efficiency of the REM/EF integrated process far exceeded the efficiency of EF and REM used as standalone processes.

Declaration of Competing Interest

The authors declare that they have no known competing financial interests or personal relationships that could have appeared to influence the work reported in this paper.

Acknowledgements

Appendix A. Supplementary data

Supplementary data to this article can be found online at https://doi.org/10.1016/j.cej.2020.125936.

References

[1] A. Joss, H. Siegrist, T.A. Ternes, Are we about to upgrade wastewater treatment for removing organic micropollutants? Water Sci. Technol. 57 (2008) 251–255, https://doi.org/10.2166/wst.2008.825.

[2] B.P. Chaplin, Critical review of electrochemical advanced oxidation processes for water treatment applications, Environ. Sci. Process. Impacts. (2014), https://doi.org/10.1039/C3EM00679D.

[3] C.A. Martínez-Huitle, M.A. Rodrigo, I. Sirés, O. Scialdone, Single and coupled electrochemical processes and reactors for the abatement of organic water pollutants: a critical review, Chem. Rev. 115 (2015) 13362–13407, https://doi.org/10.1021/acs.chemrev.5b00361.

[4] I. Sirés, E. Brillas, M.A. Oturan, M.A. Rodrigo, M. Panizza, Electrochemical advanced oxidation processes: today and tomorrow. A review, Environ. Sci. Pollut. Res. 21 (2014) 8336–8367, https://doi.org/10.1007/s11356-014-2783-1.

[5] F.C. Moreira, R.A.R. Boaventura, E. Brillas, V.J.P. Vilar, Electrochemical advanced oxidation processes: a review on their application to synthetic and real wastewaters, Appl. Catal. B: Environ. 202 (2017) 217–261, https://doi.org/10.1016/j.apcatb.2016.08.037.

[6] E. Brillas, I. Sirés, M.A. Oturan, Electro-Fenton process and related electrochemical technologies based on Fenton's reaction chemistry, Chem. Rev. 109 (2009) 6570–6631, https://doi.org/10.1021/cr900136g.

[7] M. Panizza, G. Cerisola, Direct and mediated anodic oxidation of organic pollutants, Chem. Rev. 109 (2009) 6541–6569, https://doi.org/10.1021/cr9001319.

[8] Enric Brillas, Carlos A. Martínez-Huitle, Decontamination of wastewaters containing synthetic organic dyes by electrochemical methods. An updated review, Appl. Catal. B 166-167 (2015) 603–643, https://doi.org/10.1016/j.apcatb.2014.11.016.

[9] C. Saez, R. Lopez-Vizcaino, P. Canizares, M.A. Rodrigo, Conductive-diamond electrochemical oxidation of surfactant-aided soil-washing effluents, Ind. Eng. Chem. Res. 49 (2010) 9631–9635, https://doi.org/10.1021/ie101224t.

[10] M.A. Oturan, M.C. Edelahi, N. Oturan, K. El Kacemi, J.-J. Aaron, Kinetics of oxidative degradation/mineralization pathways of the phenylurea herbicides diuron, monuron and fenuron in water during application of the electro-Fenton process, Appl. Catal. B: Environ. 97 (2010) 82–89, https://doi.org/10.1016/j.apcatb.2010.03.026.

[11] S. Garcia-Segura, E. Brillas, Mineralization of the recalcitrant oxalic and oxamic acids by electrochemical advanced oxidation processes using a boron-doped diamond anode, Water Res. 45 (2011) 2975–2984, https://doi.org/10.1016/j.watres.2011.03.017.

[12] R. Salazar, E. Brillas, I. Sirés, Finding the best Fe^{2+}/Cu^{2+} combination for the solar photoelectro-Fenton treatment of simulated wastewater containing the industrial textile dye Disperse Blue 3, Appl. Catal. B: Environ. 115–116 (2012) 107–116, https://doi.org/10.1016/j.apcatb.2011.12.026.

[13] E. Mousset, L. Frunzo, G. Esposito, E.D. van Hullebusch, N. Oturan, M.A. Oturan, A complete phenol oxidation pathway obtained during electro-Fenton treatment and validated by a kinetic model study, Appl. Catal. B: Environ. 180 (2016) 189–198, https://doi.org/10.1016/j.apcatb.2015.06.014.

[14] C. Salazar, C. Ridruejo, E. Brillas, J. Yáñez, H.D. Mansilla, I. Sirés, Abatement of the fluorinated antidepressant fluoxetine (Prozac) and its reaction by-products by electrochemical advanced methods, Appl. Catal. B: Environ. 203 (2017) 189–198, https://doi.org/10.1016/j.apcatb.2016.10.026.

[15] R.C. Burgos-Castillo, I. Sirés, M. Sillanpää, E. Brillas, Application of electrochemical advanced oxidation to bisphenol A degradation in water. Effect of sulfate and chloride ions, Chemosphere 194 (2018) 812–820, https://doi.org/10.1016/j.chemosphere.2017.12.014.

[16] E. Mousset, N. Oturan, M.A. Oturan, An unprecedented route of OH radical reactivity evidenced by an electrocatalytical process: Ipso-substitution with perhalogenocarbon compounds, Appl. Catal. B: Environ. 226 (2018) 135–146, https://doi.org/10.1016/j.apcatb.2017.12.028.

[17] M. El Kateb, C. Trellu, A. Darwich, M. Rivallin, M. Bechelany, S. Nagarajan, S. Lacour, N. Bellakhal, G. Lesage, M. Héran, M. Cretin, Electrochemical advanced oxidation processes using novel electrode materials for mineralization and biodegradability enhancement of nanofiltration concentrate of landfill leachates, Water Res. 162 (2019) 446–455, https://doi.org/10.1016/j.watres.2019.07.005.

[18] A.K. Abdessalem, N. Oturan, N. Bellakhal, M. Dachraoui, M.A. Oturan, Experimental design methodology applied to electro-Fenton treatment for degradation of herbicide chlortoluron, Appl. Catal. B: Environ. 78 (2008) 334–341, https://doi.org/10.1016/j.apcatb.2007.09.032.

[19] A. Özcan, Y. Sahin, A.S. Koparal, M.A. Oturan, A comparative study on the efficiency of electro-Fenton process in the removal of propham from water, Appl. Catal. B: Environ. 89 (2009) 620–626, https://doi.org/10.1016/j.apcatb.2009.01.022.

[20] H. Zhang, D. Zhang, J. Zhou, Removal of COD from landfill leachate by electro-Fenton method, J. Hazard. Mater. 135 (2006) 106–111, https://doi.org/10.1016/j.jhazmat.2005.11.025.

[21] M. Pimentel, N. Oturan, M. Dezotti, M.A. Oturan, Phenol degradation by advanced electrochemical oxidation process electro-Fenton using a carbon felt cathode, Appl. Catal. B: Environ. 83 (1–2) (2008) 140–149, https://doi.org/10.1016/j.apcatb.2008.02.011.

[22] O. Scialdone, S. Randazzo, A. Galia, G. Silvestri, Electrochemical oxidation of organics in water: role of operative parameters in the absence and in the presence of NaCl, Water Res. 43 (2009) 2260–2272, https://doi.org/10.1016/j.watres.2009.02.014.

[23] A. Özcan, Y. Sahin, A.S. Koparal, M.A. Oturan, Propham mineralization in aqueous medium by anodic oxidation using boron-doped diamond anode: influence of experimental parameters on degradation kinetics and mineralization efficiency, Water Res. 42 (2008) 2889–2898, https://doi.org/10.1016/j.watres.2008.02.027.

[24] C. Trellu, Y. Péchaud, N. Oturan, E. Mousset, D. Huguenot, E.D. van Hullebusch, G. Esposito, M.A. Oturan, Comparative study on the removal of humic acids from drinking water by anodic oxidation and electro-Fenton processes: mineralization efficiency and modelling, Appl. Catal. B: Environ. 194 (2016) 32–41, https://doi.org/10.1016/j.apcatb.2016.04.039.

[25] N. Oturan, S.O. Ganiyu, S. Raffy, M.A. Oturan, Sub-stoichiometric titanium oxide as a new anode material for electro-Fenton process: application to electrocatalytic destruction of antibiotic amoxicillin, Appl. Catal. B: Environ. 217 (2017) 214–223, https://doi.org/10.1016/j.apcatb.2017.05.062.

[26] E. Mousset, Y. Pechaud, N. Oturan, M.A. Oturan, Charge transfer/mass transport competition in advanced hybrid electrocatalytic wastewater treatment: development of a new current efficiency relation, Appl. Catal. B: Environ. 240 (2019) 102–111, https://doi.org/10.1016/j.apcatb.2018.08.055.

[27] C. Trellu, B.P. Chaplin, C. Coetsier, R. Esmilaire, S. Cerneaux, C. Causserand, M. Cretin, Electro-oxidation of organic pollutants by reactive electrochemical membranes, Chemosphere 208 (2018) 159–175, https://doi.org/10.1016/j.chemosphere.2018.05.026.

[28] C. Trellu, C. Coetsier, J.-C. Rouch, R. Esmilaire, M. Rivallin, M. Cretin, C. Causserand, Mineralization of organic pollutants by anodic oxidation using reactive electrochemical membrane synthesized from carbothermal reduction of TiO2, Water Res. 131 (2018) 310–319, https://doi.org/10.1016/j.watres.2017.12.070.

[29] A.M. Zaky, B.P. Chaplin, Porous substoichiometric TiO2 anodes as reactive electrochemical membranes for water treatment, Environ. Sci. Technol. 47 (2013) 6554–6563, https://doi.org/10.1021/es401287e.

[30] L. Guo, Y. Jing, B.P. Chaplin, Development and characterization of ultrafiltration TiO2 Magnéli phase reactive electrochemical membranes, Environ. Sci. Technol. 50 (2016) 1428–1436.

[31] D. Zhi, J. Wang, Y. Zhou, Z. Luo, Y. Sun, Z. Wan, L. Luo, D.C.W. Tsang, D.D. Dionysiou, Development of ozonation and reactive electrochemical membrane coupled process: enhanced tetracycline mineralization and toxicity reduction, Chem. Eng. J. 383 (2020) 123149, , https://doi.org/10.1016/j.cej.2019.123149.

[32] H. Shi, Y. Wang, C. Li, R. Pierce, S. Gao, Q. Huang, Degradation of perfluorooctanesulfonate by reactive electrochemical membrane composed of Magnéli phase titanium suboxide, Environ. Sci. Technol. 53 (2019) 14528–14537, https://doi.org/10.1021/acs.est.9b04148.

[33] S.N. Misal, M.-H. Lin, S. Mehraeen, B.P. Chaplin, Modeling electrochemical oxidation and reduction of sulfamethoxazole using electrocatalytic reactive electrochemical membranes, J. Hazard. Mater. 384 (2020) 121420, , https://doi.org/10.1016/j.jhazmat.2019.121420.

[34] G. Gao, C.D. Vecitis, Reactive depth and performance of an electrochemical carbon nanotube network as a function of mass transport, ACS Appl. Mater. Interfaces 4 (2012) 6096–6103, https://doi.org/10.1021/am301724n.

[35] R. Stirling, W.S. Walker, P. Westerhoff, S. Garcia-Segura, Techno-economic analysis

to identify key innovations required for electrochemical oxidation as point-of-use treatment systems, Electrochim. Acta 338 (2020) 135874, , https://doi.org/10.1016/j.electacta.2020.135874.

[36] J.F. Pérez, J. Llanos, C. Sáez, C. López, P. Cañizares, M.A. Rodrigo, Electrochemical jet-cell for the in-situ generation of hydrogen peroxide, Electrochem. Commun. 71 (2016) 65–68, https://doi.org/10.1016/j.elecom.2016.08.007.

[37] G. Ren, M. Zhou, M. Liu, L. Ma, H. Yang, A novel vertical-flow electro-Fenton reactor for organic wastewater treatment, Chem. Eng. J. 298 (2016) 55–67, https://doi.org/10.1016/j.cej.2016.04.011.

[38] L. Ma, M. Zhou, G. Ren, W. Yang, L. Liang, A highly energy-efficient flow-through electro-Fenton process for organic pollutants degradation, Electrochim. Acta 200 (2016) 222–230, https://doi.org/10.1016/j.electacta.2016.03.181.

[39] C. Zhang, Y. Jiang, Y. Li, Z. Hu, L. Zhou, M. Zhou, Three-dimensional electrochemical process for wastewater treatment: a general review, Chem. Eng. J. 228 (2013) 455–467, https://doi.org/10.1016/j.cej.2013.05.033.

[40] T.X.H. Le, T.V. Nguyen, Z. Amadou Yacouba, L. Zoungrana, F. Avril, D.L. Nguyen, E. Petit, J. Mendret, V. Bonniol, M. Bechelany, S. Lacour, G. Lesage, M. Cretin, Correlation between degradation pathway and toxicity of acetaminophen and its by-products by using the electro-Fenton process in aqueous media, Chemosphere 172 (2017) 1–9, https://doi.org/10.1016/j.chemosphere.2016.12.060.

[41] E. Brillas, E. Mur, J. Casado, Iron(II) catalysis of the mineralization of aniline using a carbon-PTFE O-2-fed cathode, J. Electrochem. Soc. 143 (1996) L49–L53, https://doi.org/10.1149/1.1836528.

[42] C. Flox, S. Ammar, C. Arias, E. Brillas, A.V. Vargas-Zavala, R. Abdelhedi, Electro-Fenton and photoelectro-Fenton degradation of indigo carmine in acidic aqueous medium, Appl. Catal. B: Environ. 67 (2006) 93–104, https://doi.org/10.1016/j.apcatb.2006.04.020.

[43] H. Zazou, N. Oturan, M. Sönmez-Çelebi, M. Hamdani, M.A. Oturan, Mineralization of chlorobenzene in aqueous medium by anodic oxidation and electro-Fenton processes using Pt or BDD anode and carbon felt cathode, J. Electroanal. Chem. 774 (2016) 22–30, https://doi.org/10.1016/j.jelechem.2016.04.051.

[44] E. Brillas, B. Boye, I. Sirés, J.A. Garrido, R.M. Rodríguez, C. Arias, P.-L. Cabot, C. Comninellis, Electrochemical destruction of chlorophenoxy herbicides by anodic oxidation and electro-Fenton using a boron-doped diamond electrode, Electrochim. Acta 49 (2004) 4487–4496, https://doi.org/10.1016/j.electacta.2004.05.006.

[45] S.O. Ganiyu, N. Oturan, S. Raffy, M. Cretin, C. Causserand, M.A. Oturan, Efficiency of plasma elaborated sub-stoichiometric titanium oxide (Ti4O7) ceramic electrode for advanced electrochemical degradation of paracetamol in different electrolyte media, Sep. Purif. Technol. 208 (2019) 142–152, https://doi.org/10.1016/j.seppur.2018.03.076.

[46] H. Olvera-Vargas, C. Trellu, N. Oturan, M.A. Oturan, Bio-electro-Fenton: a new combined process – Principles and applications, Electro-Fenton Process, Springer, Singapore, 2017, pp. 29–56, , https://doi.org/10.1007/698_2017_53.

[47] H. Monteil, Y. Péchaud, N. Oturan, M.A. Oturan, A review on efficiency and cost effectiveness of electro- and bio-electro-Fenton processes: application to the treatment of pharmaceutical pollutants in water, Chem. Eng. J. 376 (2019) 119577, , https://doi.org/10.1016/j.cej.2018.07.179.

[48] O. Ganzenko, D. Huguenot, E.D. van Hullebusch, G. Esposito, M.A. Oturan, Electrochemical advanced oxidation and biological processes for wastewater treatment: a review of the combined approaches, Environ. Sci. Pollut. Res. (2014) 1–32, https://doi.org/10.1007/s11356-014-2770-6.

[49] C. Trellu, O. Ganzenko, S. Papirio, Y. Pechaud, N. Oturan, D. Huguenot, E.D. van Hullebusch, G. Esposito, M.A. Oturan, Combination of anodic oxidation and biological treatment for the removal of phenanthrene and Tween 80 from soil washing solution, Chem. Eng. J. 306 (2016) 588–596, https://doi.org/10.1016/j.cej.2016.07.108.

[50] E. Brillas, I. Sirés, C. Arias, P.L. Cabot, F. Centellas, R.M. Rodríguez, J.A. Garrido, Mineralization of paracetamol in aqueous medium by anodic oxidation with a boron-doped diamond electrode, Chemosphere 58 (2005) 399–406, https://doi.org/10.1016/j.chemosphere.2004.09.028.